A Simulation Framework for the Comparison of Digital Mammography Imaging Technology

M.Yip, D. Rodriguez, E. Lewis, K. Wells and K.C. Young

***Abstract*—With the recent developments in digital mammography, it is becoming increasingly important to be able to compare different technologies used for detecting breast cancer. By using simulation tools, it may be made possible to not only compare the images generated by different technologies but also the effect of dose levels and other imaging parameters within the same system.**

Images of a test phantom (CDMAM) have been simulated in this study as a proof of principle. An image simulation chain has been devised from which various doses and other generic system parameters can be simulated. Preliminary results show that the method provides a good quality initial simulation of real CDMAM images.

***Index Terms*—Digital mammography, CDMAM phantom, simulation**

I. Introduction

A wide variety of digital mammography systems are now available. However these vary greatly in terms of physical performance and cost; ranging from expensive direct digital mammography systems (DR) to less expensive computerised radiography (CR) systems. The more expensive systems generally have better physical characteristics, but the impact of this on clinical performance is unknown. There is therefore a need to assess the effect of physical characteristics on clinical outcomes. Standard methods of measuring the physical performance of digital detectors are well established (e.g. modulation transfer function (MTF) and noise power spectrum (NPS)). However the relationship between such measures and clinical results is not well understood. Currently minimum and acceptable standards of image quality in the UK and Europe are based on measurements with a test object (CDMAM). However, it remains unclear how the results of such tests relate to clinical results. Clinical trials are too expensive and time consuming to enable detailed comparisons between multiple systems or ways of operating those systems.

In order to investigate the optimum detector technology and acquisition protocol, to achieve effective diagnosis of breast cancer, comparison of clinically realistic images from different detectors is needed. A simulation procedure for generating realistic images of breast cancer would be a powerful method for measure of the performance of radiologists and CAD systems in detecting cancers when different systems, radiation doses, beam qualities and image processing is used.

In this work, a framework for simulating images produced by a digital mammography detector has been developed and evaluated. The framework is able to simulate images based on image quality metrics such as MTF and NPS, and other factors such as heel effect and exposure settings. The simulation of the imaging chain has been validated using images of the CDMAM mammography test phantom.

The CDMAM phantom (Figure 1) is widely used to evaluate the performance of a mammography systems and forms the basis of European image quality standards. It is a contrast-detail test object designed to assess the imaging system's ability to distinguish very fine and low contrast details. Although the flat background of the CDMAM phantom represents a highly simplified case compared to real clinical breast images[1], it represents a highly responsive assessment system. This phantom has been made the subject of this simulation study as a proof of principle. It consists of an array of cells each containing two gold discs. The observer has to attempt to identify the location of the corner disc in each cell. This is a very time consuming task, but automated CDMAM scoring software is available[2].

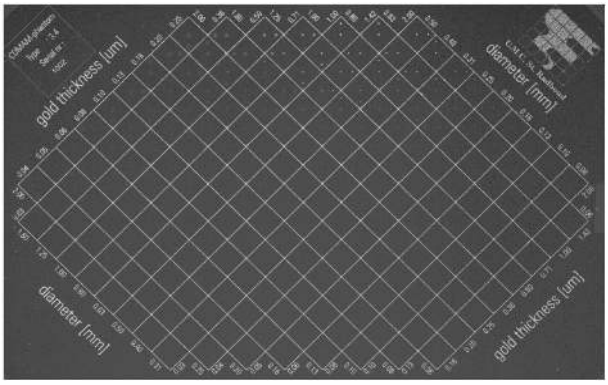

Fig. 1. Radiographic image of a CDMAM phantom.

II. Method

Several factors need to be taken into account in order to successfully simulate a mammographic image. Image quality metrics such as MTF and NPS can be used to describe an imaging system. This evaluation considers the resolution and noise properties of the simulated images. The impact of other factors such as the choice of tube voltage, and target/filter material, which affect the contrast of objects in the image,

Manuscript received November 16, 2007. This work was supported by the EPSRC.

M.Yip, D.Rodriguez, E.Lewis and K.Wells are from Centre for Vision, Speech and Signal Processing, Faculty of Engineering and Physical Sciences, University of Surrey, Guildford, Surrey GU2 7XH, UK.

email:M.Yip@surrey.ac.uk

K.C.Young is from UK Coordinating Centre for the Physics of Mammography, Royal Surrey County Hospital, Guildford, Surrey, GU2 7XX, UK

will be added later. The method used to simulate the imaging chain is illustrated in Figure 2.

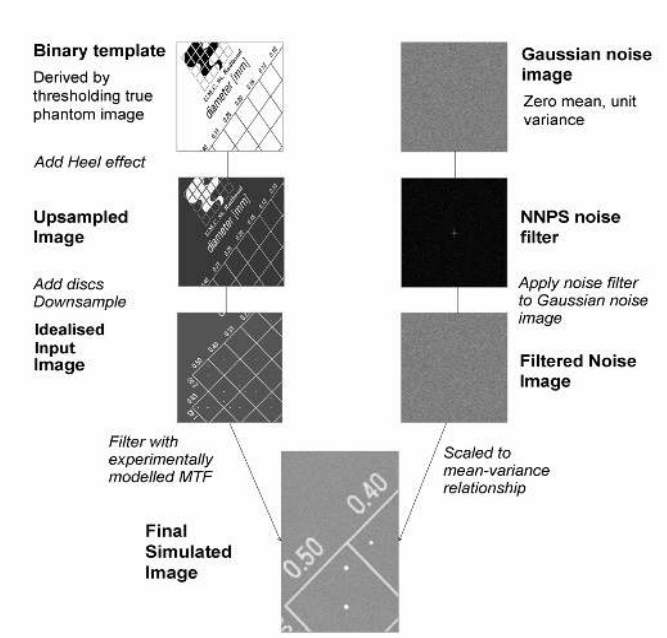

Fig. 2. Imaging chain for the simulation of images from a digital mammography detector. The binary template is created from a high-dose CDMAM image. Intensity values are added to this image before being highly sampled. Discs are added to the image and downsampled to the final resolution, $70\mu m$ in this case. The image is then filtered with an experimentally measured MTF. A noise image is created through filtering a Gaussian noise field through an NNPS filter. The noise image and blurred idealised input image are added together to produce the final simulated CDMAM image.

A. Simulation

1) Generating an Ideal Image: The simulation starts with a high-dose image of the CDMAM test object obtained using a commercial imaging system. The background details such as the grid pattern and insignias in the phantom are assumed to have the same pixel intensity. Intensities for the background were assigned as measured experimentally for different doses. Data sets for four dose levels were available (22mAs, 55 mAs, 110mAs, 220mAs).

2) Adding the Heel effect: The heel effect is inherent in radiography systems due to non-uniformity in the X-ray beam, and causes a characteristic slow varying intensity across each image. To add the heel effect to the image, a mask derived from a high-dose CDMAM image was used. The mask was created by applying a median filter of 300x300 pixels to a high-dose CDMAM image, to leave the slow varying shape of the heel effect. This filter was chosen as it was twice the diameter of a cell in the array, thus ensuring that the grid pattern did not distort the measurement of the heel effect. The heel effect mask, I_{heel}, was applied to the input image, I_{input} to produce an idealised input image as shown in (1)

$$Im_{idealised} = (Im_{heel}/\mu_{heel}) * Im_{input} \quad (1)$$

where μ_{heel} is the mean pixel value obtained from Im_{heel}. To allow for applicability with other systems with different resolution, Im_{heel} was upsampled with bilinear interpolation to $10\mu m$ per pixel.

3) Inserting discs: The pixel intensity was assigned for each disc based on the gold thickness specified by the manufacturer and measurements of the contrast of some of the discs. A region of interest (ROI) was placed within the centre of the largest disc (2mm diameter) for each gold thickness, taking care to avoid blurring effects at the edges of the disc, to measure the disc's mean central pixel intensity, I_{disc}. A number of ROIs were placed around the disc to measure the background pixel intensity, $I_{background}$. The relative contrast was calculated as in (2).

$$C = (I_{background} - I_{disc})/I_{background} \quad (2)$$

where $I_{background}$ and I_{disc} were corrected for the offset ϕ inherent.

This contrast was compared with theoretical calculations for the same setup of CDMAM image acquisition in Figure 3. The radiographic contrast was calculated for the spectrum expected when using a tube voltage of 32kVp and a Molybdenum/Rhodium target/filter material combination for the test phantom configuration. This includes a 4cm thick slab of polymethyl methacrylate (PMMA) with a further 3mm thickness of PMMA for the CDMAM phantom and its 0.5mm thick aluminium backing plate and the varying thickness for the gold discs. Deviations from the theoretical values may be accounted by measurement error and contrast degradation due to scatter. The contrasts of the discs are compared with the contrast calculated using the theoretical model adjusted for contrast degradation due to scatter in Figure 3.

The highly sampled 'ideal' image was next downsampled to the pixel dimensions of the imaging detector to be simulated using bilinear interpolation, leaving an idealised input image.

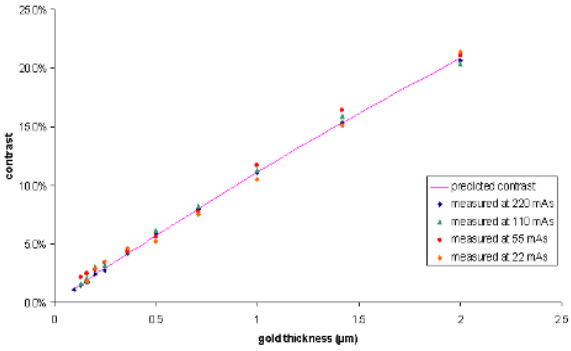

Fig. 3. Relationship of contrast as a function of disc thickness as measured empirically (solid line) compared with theoretical values (dashed line) with 32kVp, Molybdenum/Rhodium target/filter material.

4) Resolution modification: The MTF of the system to be simulated was measured with a sharp edge image acquired with the system[3]. This experimentally measured MTF was

smoothed before using bicubic interpolation in two dimensions, assuming this is isotropic, such that it could be evaluated at any arbitrary point[4]. The idealised input image was transformed into Fourier space using a two-dimensional Fast Fourier Transform (FFT). The modelled MTF was multiplied directly with the Fourier Transformed idealised input image, $Im_{idealised}$. An inverse two-dimensional FFT, $\mathfrak{F}_2^{-1}$, of this output created a real space filtered image, $Im_{blurred}$ as defined in (3).

$$Im_{blurred} = \mathfrak{F}_2^{-1}(\mathfrak{F}_2(Im_{idealised}).MTF) \tag{3}$$

5) Noise simulation: In order to create noise in the frequency domain, as outlined by previous authors [4], [5], [6], [7], a noise filter is required. This noise filter is unique to the detector system and it is assumed to be uniform across all dose levels [6] as it is based on the NNPS (Normalised NPS) of the imaging system itself as defined in (4).

$$NNPS(u_n, v_k) = \lim_{N_x, N_y, M \to \infty} \frac{\Delta x \Delta y}{M N_x N_y} \sum_{m=1}^{M} \left| \sum_{i=1}^{N_x} \sum_{j=1}^{N_y} \left[Im(x_i, y_j) - \bar{Im} \right] e^{-2\pi i (u_n x_i + v_k y_j)} \right|^2 \tag{4}$$

A noise filter was based on the square root of the input NNPS . The NNPS was extracted from a uniform image acquired on the system using a 4cm thick slab of PMMA. The NNPS was measured using an ensemble of 256x256 pixel ROIs within a region of ∼7cm x 7cm located within the centre of the image such that it was not affected by the non-uniformity of scatter on the periphery of the image. The resultant NNPS was interpolated using bicubic methods such that it could be evaluated at any point. This noise filter was multiplied by a Fourier representation of Gaussian white noise, Im_G, with zero mean and unit variance, to create a noise image, Im_{noise} as defined in (5). This ensures that the overall mean of the image is not altered when the noise image is added.

$$Im_{noise} = \mathfrak{F}_2^{-1}(\mathfrak{F}_2(Im_G).\sqrt{NNPS}) \tag{5}$$

The noise was inverse Fourier Transformed back into real space and scaled following a mean-variance relationship, $\sigma(I_{blurred}(x, y))$, on a pixel-by-pixel basis as defined in (6).

$$Im_{scalednoise}(x, y) = Im_{noise}(x, y).\sqrt{\sigma(Im_{blurred}(x, y))} \tag{6}$$

This scaled noise image added to the idealised input image as defined in (7), where the simulated image, Im_{sim}, is the sum of the filtered image, $Im_{blurred}$, and the scaled noise image, $Im_{scalednoise}$.

$$Im_{sim} = Im_{blurred} + Im_{scalednoise} \tag{7}$$

The result of this simulation is illustrated in Figure 4. Figure 5 illustrates the step-by-step process of the image simulation chain from the ideal image (Figure 5a) to the blurred image (Figure 5b) to the final simulated image with noise added (Figure 5c) for two disc diameters.

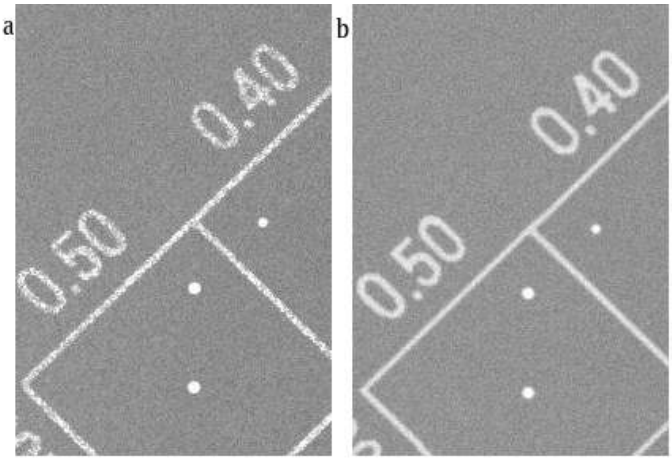

Fig. 4. a) Cropped part of a real CDMAM image acquired at a high dose level and b) corresponding part of simulated CDMAM the same dose level.

B. Validation of the Simulated Images

Validation of the simulation was achieved by comparing the simulated images with the real images. This included the relative noise of the background in the real and simulated CDMAM images. Statistical measurements have been made in relatively uniform areas of the CDMAM image, away from the periphery to avoid the heel effect, with a number of 55x55 pixel ROIs. In order to work with the pixel values that are linear with absorbed detector dose, an offset inherent to this type of detector was subtracted before making any calculations as in equation (8)

$$N_{rel} = \frac{\sigma}{\mu - \phi} \tag{8}$$

Where the relative noise,N_{rel}, is given by the ratio of standard deviation, σ, to the mean, μ, taking account of the offset, ϕ. MTF validation was carried out with a synthetic edge image, produced with the image simulation chain as described in Figure 1. The MTF calculated from this synthetic edge image is compared with its original counterpart in Figure 7. NNPS measurements of the simulated image were carried out with a synthetic uniform image produced with the image simulation chain. This has also been compared with its real counterpart in Figure 8.

Further investigation of the effects of the blurring and noise was carried out with the use of surface plots for individual simulated discs. Simulated images of discs of 0.13mm and 0.5mm diameter were compared with their corresponding real images with the use of surface plots and line profiles.

III. Results

Figure 6 shows how the relative noise varied with pixel value taken at four doses. The relative noise measured for real and simulated images were comparable, at the four dose levels. This a best fit of the data lead to a value of n = -0.48. An index value of 0.5 would be expected for a quantum noise limited system bearing in mind that the pixel value has been linearised to be proportional to energy deposition.

The NNPS of the simulated CDMAM image is compared to the real CDMAM image in Figure 7 showing close agreement.

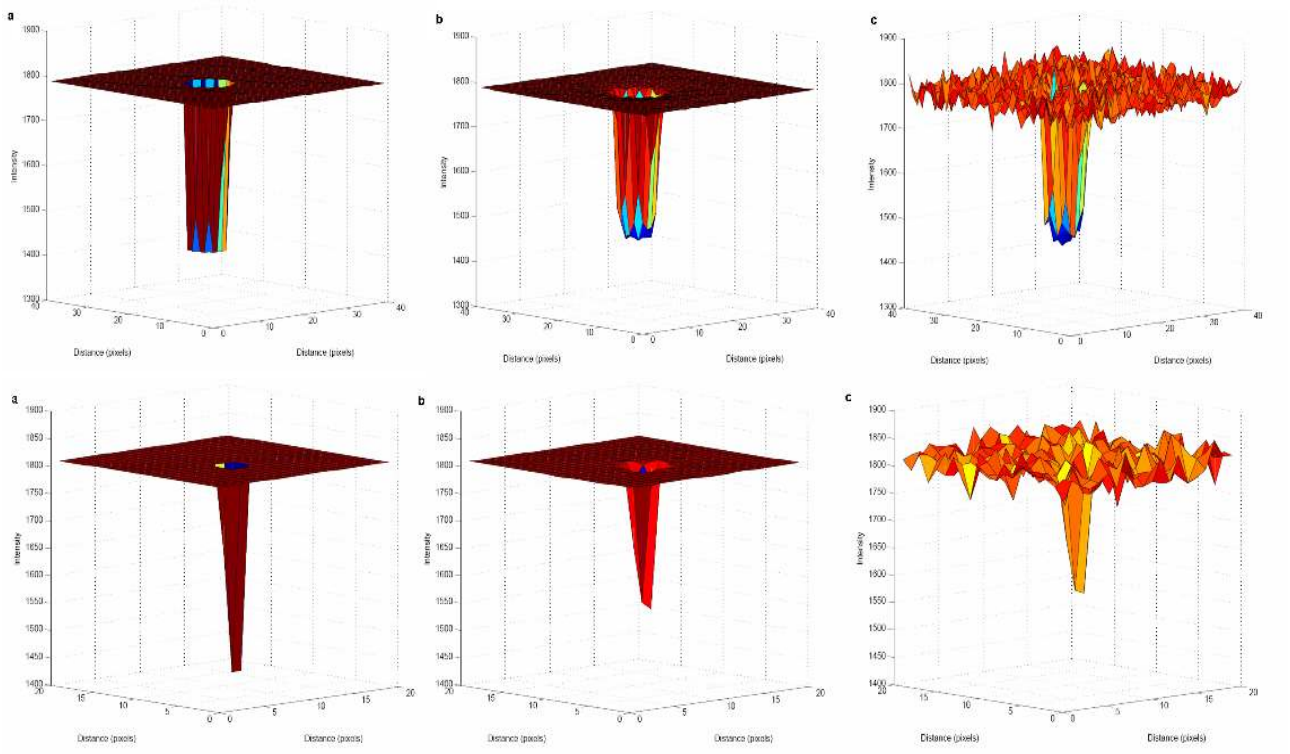

Fig. 5. Surface plots of 0.5mm and 0.13mm diameter discs (top and bottom respectively) at different stages of simulation, (a) idealised input image $Im_{idealised}$, (b) blurred image $Im_{blurred}$, (c) final simulated image Im_{sim}.

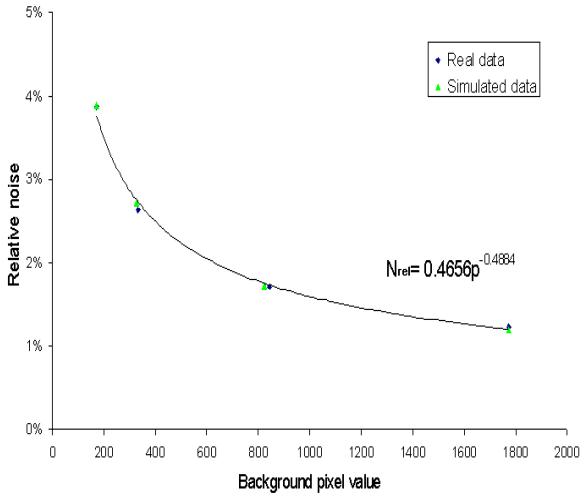

Fig. 6. Relative noise against background pixel value. The real values are in diamonds, whilst the simulated values are plotted with triangles. The line gives a best fit to the data, relating N_{rel} to the pixel value, p.

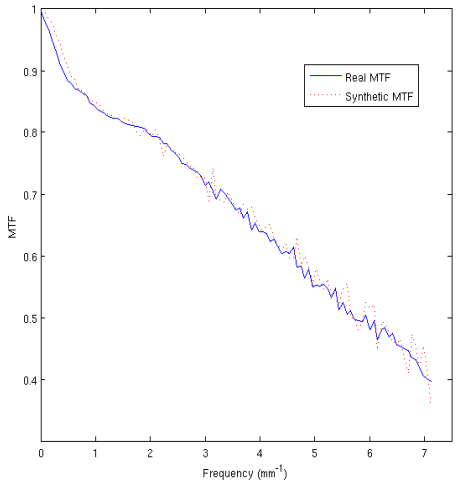

Fig. 7. Presampled MTF for a simulated edge image compared with measured MTF of the detector.

The presampled MTF from a sharp simulated edge image is displayed in Figure 8 with the presampled MTF of the real system. The two curves show close agreement.

Direct comparison with the real image was made in Figure 9 using a line profile (Figure 9c). The contrast levels for both discs in relation to the background have been successfully simulated.

IV. Discussion

Initial results are promising. The relative noise for images at each dose level have been comparable with that measured in the corresponding real images. The image simulation chain provides a useful method for comparing the effects of MTF and NPS on individual details such as the discs in Figure 5 using a step-by-step approach. The final simulated image was compared with its real counterpart for validation in Figure 9.

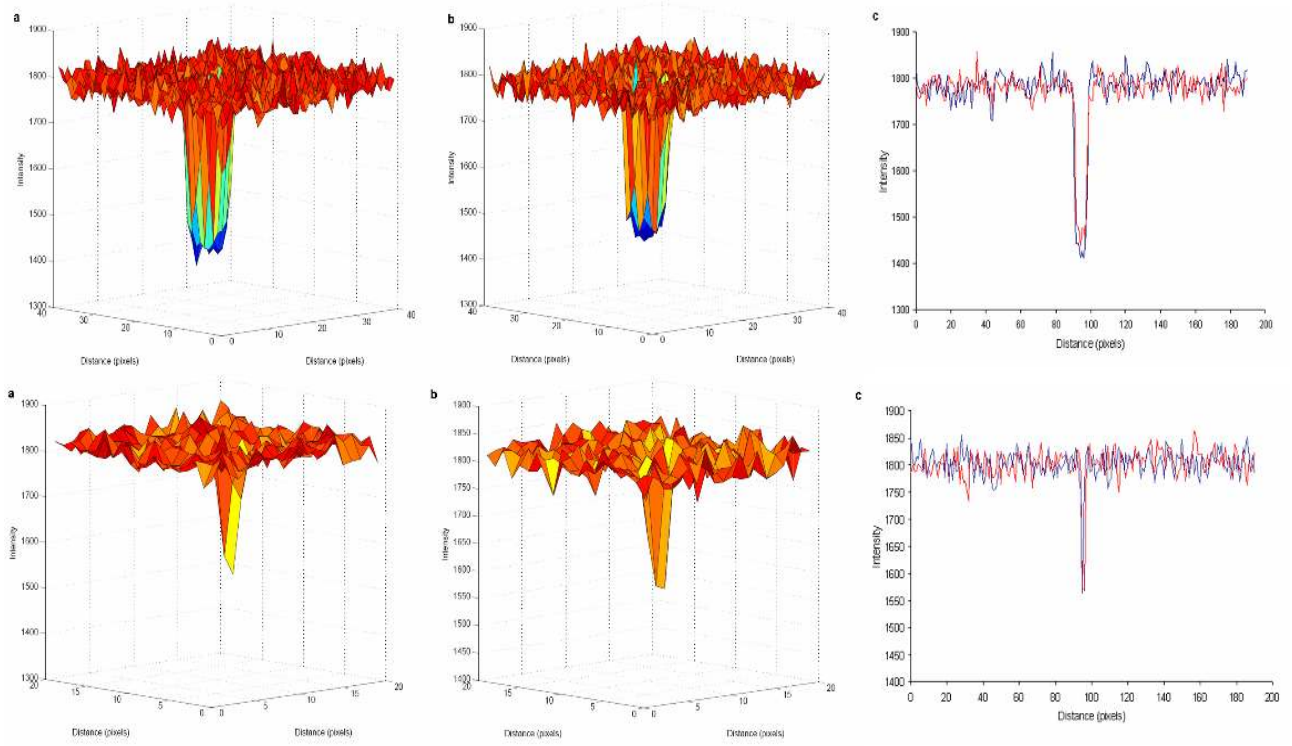

Fig. 9. 0.5mm and 0.13mm diameter discs (top and bottom respectively) (a) surface plot of real disc, (b) surface plot of simulated disc, Im_{sim}, (c) line profile comparisons of the same disc. The blue line shows the profile of the real data whilst the red line shows the profile of the simulated data.

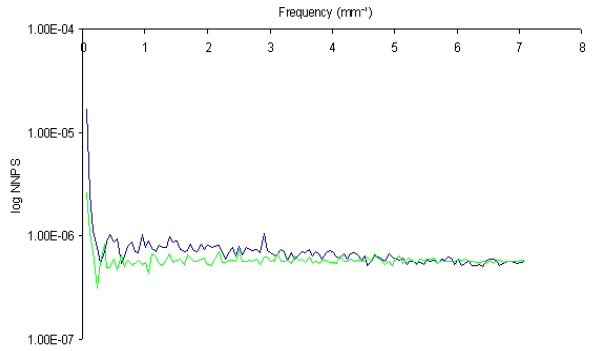

Fig. 8. 1D NNPS profiles for real (blue) and simulated (green) images.

Both discs had comparable background and disc pixel values, which was verified with the line profile.

The NNPS profiles showed a close match between real and simulated images. The MTF modelled directly on the measured edge data yielded a very close match the original MTF used to form the simulated images.

The method described here starts from a noiseless idealised image, which is appropriate for a simplistic test object such as the CDMAM. However, further application to clinically relevant images, such as real mammograms, will have to take into account the MTF and NPS properties of the original system before applying those to be simulated. Further work will be needed to refine the model to take account of some additional factors such as beam qualities, different detectors etc.

The image simulation framework has demonstrated a method of creating digital mammographic images based on image quality metrics, such MTF and NPS.

REFERENCES

[1] B. Grosjean and S. Muller. Impact of textured background on scoring of simulated cdmam phantom. In Susan M.Astley et al, editor, *IWDM 2006, LNCS 4046*, pages 460–467. LNCS, Springer-Verlag Berlin Heidelberg, 2006.

[2] R. Visser and N. Karssemeijer. Manual cdcom version 1.5: software for automated readout of cdmam 3.4 images. *Available with CDCOM software at www.euref.org*, 2007.

[3] E. Buhr, S. Günther-Kohfahl, and U. Neitzel. Accuracy of a simple method for deriving the presampled modulation transfer function of a digital radiographic system from an edge image. *Med. Phys.*, 30(9):2323–2331, 2003.

[4] R.S. Saunders and E. Samei. A method for modifying the image quality parameters of digital radiographic images. *Med. Phys.*, 30(11):3006–3017, 2003.

[5] M. Båth, M. Håkansson, A. Tingberg, and L.G. Månsson. Method of simulating dose reduction for digital radiographic systems. *Radiation Protection Dosimetry*, 114(1-3):253–259, 2005.

[6] A-K. Carton, H. Bosmans, D. Vandenbroucke, G Souverijns, C.V. Ongeval, and G. Marchal. Quantification of al-equivalent thickness of just visible microcalcifications in full field digital mammograms. *Medical Physucs*, 2004.

[7] A. Workman. Simulation of digital mammography. volume 5745, pages 933–942, Bellingham, WA, 2005. SPIE.